

Active control of helicopter blade stall

Khanh Nguyen

NASA, Ames Research Center, Moffett Field, CA

AIAA, Dynamics Specialists Conference, Salt Lake City, UT, Apr. 18, 19, 1996

This paper describes the numerical analysis of an automatic stall suppression system for helicopters. The analysis employs a FEM and includes unsteady aerodynamic effects (dynamic stall) and a nonuniform inflow model. The stall suppression system, based on a transfer matrix approach, uses blade root actuation to suppress stall directly. The results show that stall can effectively be suppressed using higher harmonic blade root pitch at both cruise and high speed flight conditions. The control amplitude was small, less than 1 deg. In a high thrust, low speed flight condition, stall is fairly insensitive to higher harmonic inputs. In general, stall suppression does not guarantee performance improvements. The results also show the distinction between stall suppression and performance improvement with active control. When the controller aims to reduce the shaft torque, rotor performance improvement can be achieved with a small degradation in stall behavior. (Author)

ACTIVE CONTROL OF HELICOPTER BLADE STALL

Khanh Nguyen*

NASA Ames Research Center, Moffett Field, CA

Abstract

This paper describes the numerical analysis of an automatic stall suppression system for helicopters. The analysis employs a finite element method and includes unsteady aerodynamic effects (dynamic stall) and a nonuniform inflow model. The stall suppression system, based on a transfer matrix approach, uses blade root actuation to suppress stall directly. The results show that stall can effectively be suppressed using higher harmonic blade root pitch at both cruise and high speed flight conditions. The control amplitude was small, less than 1 deg. In a high thrust, low speed flight condition, stall is fairly insensitive to higher harmonic inputs. In general, stall suppression does not guarantee performance improvements. The results also show the distinction between stall suppression and performance improvement with active control. When the controller aims to reduce the shaft torque, rotor performance improvement can be achieved with a small degradation in stall behavior.

Introduction

Suppression of retreating blade stall has been proposed as a means of helicopter flight envelope expansion, thereby enhancing the utility of these aircraft. Unlike fixed-wing aircraft, stall does not limit the low speed operation of helicopters. Stall on rotor blades, however, limits the helicopter maximum speed as well as the loading capabilities. Stall places a loading limit on most of the helicopter flight envelope at low and medium speed, and at high speed, either stall or compressibility effects can limit helicopter operations. A rotor experiencing stall can require more shaft power than is available from the engine. Also, the excessive control loads on a stalled rotor blade, together with the changes in blade aerodynamic behavior, adversely affect aircraft handling qualities. Stall-induced loads, possibly in combination with blade dynamics as in stall flutter, can severely damage blade structural components and cause excessive cabin vibration.

A unique characteristic of helicopter stall is the occurrence of stall on the retreating side of the rotor disk. In

forward flight, a blade encounters a different dynamic pressure due to the combination of blade rotation and rotor translation speed. Thus, the dynamic pressure is greater on the advancing side than on the retreating side. For roll moment balance, the blade operates at angles of attack that are low on the advancing side and high on the retreating side. At high blade loading or at high forward speeds, the local blade section angle of attack can become large enough to stall. For untwisted blades, the stall area occurs near the blade tip, growing inboard as the loading or the forward speed increases [1]. For twisted blades, the effects are reversed -- the stall area spreads from the blade root outboard.

Operating in an unsteady environment, the most severe type of stall encountered by a rotor blade is dynamic stall. In forward flight, the blade experiences time-varying dynamic pressure and angle of attack changes arising from blade pitch inputs, blade elastic response, and non-uniform rotor inflow. If supercritical flow develops under dynamic conditions, then dynamic stall is initiated by leading edge or shock-induced separation. Supercritical flow is associated with the bursting of the separation bubble as the bubble encounters the large adverse pressure gradient near the blade leading edge [2]. Dynamic stall is characterized by the shedding of strong vortices from the leading edge region. The leading edge vortex produces a large pressure wave moving aft on the airfoil upper surface and creating abrupt changes in the flow field. The pressure wave also contributes to large lift and moment overshoots in excess of static values and significant nonlinear hysteresis in the airfoil behavior.

The other type of stall typically encountered by rotor blades involves trailing edge separation. The phenomenon of trailing edge separation is associated with either static or dynamic conditions. Separation starts from the airfoil trailing edge, and with increasing angle of attack, the separation point progresses towards the leading edge region. Trailing edge separation contributes to nonlinear behavior, such as hysteresis, in lift, drag and pitching moment due to the loss in circulation. In contrast to dynamic stall that is characterized by abrupt changes in airfoil behavior, trailing edge stall progresses at a moderate rate.

Passive control of blade stall typically involves the tailoring of blade twist and planform for efficient blade load distribution. Another method employs blade construction with multi-airfoil sections -- thick, high-lift sections inboard and thin, transonic sections for the tip re-

*Aerospace Engineer

gion. These methods aim to provide efficient rotor disk loading and low drag and thus, employed primarily for performance benefits; however, they also provide stall alleviation.

As an alternative to passive methods, active control of blade pitch has the potential to alleviate blade stall. Recent development of high-frequency, blade-mounted actuators [3] makes this concept feasible. The operating frequencies for blade pitch control are not limited by the blade-integer harmonics, as in swashplate oscillation, but by the bandwidth of the actuators. Recently, ZF Luftfahrttechnik, GmbH of Germany built and wind tunnel tested, together with NASA Ames Research Center, an individual-blade-control system on a full-scale BO-105 rotor. These actuators were tested at harmonics from 2P to 6P (42.5 Hz) and amplitudes up to 3 deg. Although no stall suppression study was attempted, the benefits of IBC input on rotor performance at high forward speed (advance ratio $\mu = 0.4$) were encouraging [3].

Previous Work

In 1952, Stewart [4] suggested that two per-rev (2P) blade pitch applied to rotors in forward flight could be used to delay the onset of retreating blade stall. Based on the analysis that included a rigid flapping blade, quasi-steady aerodynamics and uniform inflow models, Stewart derived an approximate transfer function relating the change in 2P blade angle of attack due to 2P control. Results indicated that rotor disk loading could be efficiently re-distributed using higher harmonic blade pitch. For a particular flight condition, the loading redistribution could be adjusted to avoid retreating blade stall. The resulting effects would be to raise the speed limitation of helicopters. According to his analysis, the helicopter speed limit could be increased by 0.1 in advance ratio. However, Stewart did not consider the power requirement due to the speed increase.

Payne expanded Stewart's results to include the effects of active control using input harmonics higher than 2P [5]. He argued that 2P control alone would not be sufficient to raise the speed limitation of helicopters, but a combination of the second and higher harmonic control would be more effective. In the process, Payne derived generalized transfer functions relating changes in blade angle of attack to the higher harmonic control of a hovering rotor. However, Payne did not quantify the speed limit gain from his approach.

Arcidiacono conducted a numerical simulation to study the effects of second and higher harmonic control on stall [6]. This numerical analysis was more accurate and included more realistic modeling of physical phenomena than previous analyses. The analysis was capable of including the effects of static stall and Mach number in the form of two-dimensional airfoil tables. Based on the

computed transfer functions relating higher harmonic control to changes in blade angle of attack, Arcidiacono derived a blade pitch schedule that approximated an "ideal schedule" for stall alleviation. The analysis showed that the blade pitch schedule, which included both 2P and 3P components with a combined maximum amplitude of 4.3 deg, was capable of avoiding retreating blade stall. The resulting effects could raise the speed limit of a helicopter by 30 percent over the baseline maximum speed. The additional power requirement due to the speed gain would be large, however, to compensate for the increase in fuselage and rotor profile drag (about 100 percent).

In 1961, a flight test program was conducted to investigate the feasibility of using higher harmonic control on an UH-1A helicopter [7]. Using a rotor head mechanism capable of generating 2P blade pitch, Bell Helicopter conducted a series of flight tests to determine the effects of active control on rotor performance and loads. Test results indicated that the 2P control at different amplitudes and phases did not produce any reduction in rotor shaft torque. Determined to resolve this variance with theoretical prediction, the investigators conducted a post-test analysis. Analytical results indicated that the drag reduction in the retreating side due to 2P control was offset by an increase in profile drag in the fore and aft portions of the rotor disk. Such conclusions confirmed previous analytical predictions that 2P control could reshape the rotor disk loading.

Kretz [8, 9] reported the wind tunnel test results of a Stall Barrier Feedback (SBF) system on a six-foot diameter two-bladed rotor. The salient feature of the system was the ability to detect and, through feedback control, prevent blade stall. The SBF system employed three pressure sensors mounted at the 85 percent blade radial station and high-bandwidth hydraulic actuators to control each blade. The pressure sensors provided feedback signals that activated the actuators in an attempt to prevent stall. The system was configured such that once the leading edge pressure exceeded a threshold value, the actuators became active, generating a sharp pulse (e.g., an 8 deg nose down pulse was generated within 75 deg of rotor azimuth) to reduce the blade pitch. The threshold pressure value had been inferred from experimental data and used as an indicator of stall onset. Limited stall avoidance was achieved with the SBF system, which resulted in some lift gain. Most significant was the performance gain -- an 8 percent reduction in shaft torque -- for the rotor operating at an advance ratio of 0.3 and blade loading (C_T/σ) of 0.1. However, it was unclear whether the rotor was re-trimmed after the application of active control to maintain identical rotor operating conditions.

As a leading advocate in individual-blade-control (IBC), Ham has also conducted experiments in active stall suppression. The methods of sensing stall, however, dif-

ferred from that of Kretz. In one experiment reported by Ham and Quackenbush [10], the controller sensed the blade pitch motions to modify the blade torsion dynamics, and the feedback gain was adjusted to increase blade torsion damping. The increase in damping would prevent stall flutter, an indicator of retreating blade stall. The experiment was conducted in a non-rotating mode and thus, was not validated in a simulated helicopter environment. In another experiment performed by McKillip [11], the controller successfully reduced 5P blade inplane accelerations, used as an indicator of retreating blade stall.

Scope of Current Investigation

The objective of the current study is to evaluate the effectiveness of an automatic stall suppression system for helicopters using higher harmonic blade root input. The effects of stall suppression on rotor performance and the control authority required are also investigated.

An advanced rotorcraft analysis, capable of modeling the aeroelastic response of elastic blades, dynamic stall, and non-uniform rotor inflow, is adopted and modified for this active control study. The nonlinear controller development is based on a transfer matrix approach with the option for matrix updating at each controller cycle. The effect of stall reduction on rotor performance is investigated. The results quantify the distinction between control of stall versus control for performance gain.

Two aspects of the present study are unique. First, stall suppression is formulated as an optimization problem in which the stall behavior of a rotor is quantified and subsequently minimized using higher harmonic control (HHC). Thus, the system suppresses stall directly. Second, the range of flight conditions considered varies from low to high speed flight, which helps evaluate the effectiveness of higher harmonic control for stall suppression when different physical phenomena dominate the rotor flow field, e.g., low speed stall versus high speed shock-induced separation.

In this paper, the term higher harmonic control refers to blade pitch input with harmonic contents greater than one per-rev. Since the focus of the paper is on the aerodynamic performance aspects of stall suppression, the effects of HHC on blade loads, control system loads, and vibratory hub loads, which can be significant, are not discussed.

Description of Analysis

Aeroelastic analysis

Since accurate representation of the blade aeroelastic responses to the complex rotor flow field, together with a robust and accurate numerical method for blade response

solution, is mandatory for the analysis of stall control, the Ames-modified version of the University of Maryland Advanced Rotorcraft Code (UMARC) [12] is adopted for this investigation. UMARC/A is a finite element code that includes advanced unsteady aerodynamics and vortex-wake modeling. The structural and aerodynamic modeling of UMARC/A makes the code an appropriate tool for studying active control effects on rotor behavior.

The rotor blade is modeled as an elastic, isotropic Bernoulli-Euler beam undergoing small strain and moderate deflections. The blade degrees of freedom are flap bending, lead-lag bending, elastic twist, and axial deflections. The finite-element-method based on Hamilton's principle allows a discretization of the blade model into a number of beam elements, each with fifteen degrees of freedom.

The blade airloads are calculated using a nonlinear unsteady aerodynamic model based on the work of Leishman and Beddoes [13]. This model consists of an attached compressible flow formulation along with a representation of the nonlinear effects due to trailing edge separation and dynamic stall. In the attached flow formulation, the normal force (or lift) and pitching moment includes both circulatory and impulsive (noncirculatory) components. Physically, the circulatory components model the shed wake effects, while the impulsive components originate from the pressure wave generated by the airfoil motion. For dynamic stall modeling, an artificial normal force c_N' is computed based on the attached flow lift and the dynamics of the pressure distribution, represented by a time-lag model. This quantity incorporates the effects of stall delay and is used in a criterion of stall onset.

The trailing edge separation model is based on Kirchhoff's formulation that relates the separation point f to the airfoil force and moment behavior. The variation of the separation point with angle of attack is constructed from static airfoil data, then the results are curve-fitted using five parameters. The separation point value is a measure of the degree of nonlinearity in the lift behavior. Information about the flow separation point also allows the reconstruction of the airfoil static behavior, a precursor to the modeling of the airfoil dynamic characteristics.

For dynamic stall, the stall onset is based on the criterion such that the leading edge separation initiates only when the artificial normal force c_N' attains a critical value, c_{N1} , corresponding to a critical leading edge pressure. In this model, c_{N1} is the airfoil maximum static lift coefficient (available from airfoil tables) and is a function of the Mach number. Once initiated, the excess lift due to dynamic stall is governed by the dynamics of the vortex lift, defined as the difference in lift between the attached (linear) and separated flow (nonlinear)

regimes. The vortex movement over the airfoil upper surface induces a large change in the pitching moment. The vortex induced pitching moment is computed based on the vortex lift and the position of the center of pressure.

For the inflow calculation, a prescribed wake model is used for the high speed flight condition, and a modified free wake model is used for the low speed flight condition. Both wake models are originally adapted from CAMRAD [14]. A modification to the free wake model improves the convergence behavior of the wake geometry computation by using a predictor-corrector updating scheme with non-reflective periodic boundary conditions.

The coupled blade responses and trim control settings are solved for simulated wind tunnel conditions. For trim, the rotor shaft orientation is prescribed, and the blade collective and cyclic pitch inputs are automatically adjusted to desired values of thrust and hub moments. A modal reduction technique is employed in the blade response solution to reduce the computational requirement. The modal equations are solved iteratively using a robust finite-element-in-time method in which the periodic boundary conditions are inherent in the formulation. The converged solution satisfies the governing equations for both rotor trim and blade responses, which include higher harmonic control effects.

Higher Harmonic Control System

The controller algorithm, based on a transfer function matrix approach, is implemented in UMARC/A. Depending on the control objectives considered -- to suppress stall or to reduce rotor shaft torque -- each element of the transfer matrix represents the sensitivity of the controlled parameter (z) to each harmonic of the blade root actuation (u). In this investigation, the transfer matrix is computed using a finite-difference-method in which each harmonic of the control input (sine and cosine components) is perturbed individually. The control law is formulated as an optimization problem:

$$\min (qz_i^2 + u_i^T R u_i) \quad (1)$$

subjected to

$$z_i = z_{i-1} + (1-r)T_i(u_i - u_{i-1}) \quad (2)$$

For stall suppression, z_i is the stall index computed at each controller cycle by:

$$z_i = \sum_m^{24} \sum_n^{120} F(r_m, \psi_n) \quad (3)$$

where the double summation is over the 2880 airload computation points over the rotor disk (24 points in the radial direction \times 120 azimuth steps), and

$$F(r, \psi) = \begin{cases} (c_N' - c_{N1})M^2 & \text{if } c_N' \geq c_{N1} \\ 0 & \text{otherwise} \end{cases} \quad (4)$$

Note that F is defined over the rotor disk, with r being the blade radial station and ψ the azimuth angle. With this definition, the stall index is a metric that measures the severity of stall on the rotor disk in term of the excess lift over the stall area. The excess lift is the amount of artificial lift c_N' over the airfoil maximum lift c_{N1} , adapted from the dynamic stall model described earlier.

In Eq. 2, the control rate factor r , with value between 0 and 1, limits the control update rate, and i denotes the controller cycle. The transfer matrix updating is an option in which T_i is updated at each controller cycle, based on a secant method [15]. The T matrix updating, when used in combination with the control rate limit, helps improve the convergence of the controller when nonlinear effects dominate. This approach was successfully applied to another control problem -- vibration suppression of rotors under stalled conditions [16] -- with significant nonlinearity in the model.

The vector u_i represents the control input that includes harmonics from 2 to 6 per rev:

$$u_i = [\theta_{2c} \quad \theta_{2s} \quad \dots \quad \theta_{6c} \quad \theta_{6s}]^T \quad (5)$$

In terms of the elements of u_i , the higher harmonic schedule for the j th blade for is:

$$\theta_{HHC}^j(\psi) = \sum_{k=2}^6 A_k \cos(k\psi^j - \phi_k) \quad (6)$$

where the amplitude is:

$$A_k = \sqrt{\theta_{k,c}^2 + \theta_{k,s}^2} \quad (7)$$

and the phase is:

$$\phi = \tan^{-1} \left(\frac{\theta_{k,s}}{\theta_{k,c}} \right) \quad (8)$$

In Eq. 1, the factors q (scalar) and R (diagonal matrix) are used to place relative weightings to the controlled param-

eter z_j and each component of the input vector, respectively.

Besides stall suppression, a second controller is also investigated. This controller aims to improve the rotor performance using higher harmonic blade root pitch. For this system, the controlled parameter (Eq. 3) is simply the rotor shaft torque. Except for the change in the definition of z , this controller retains the same structure as that of the stall suppression controller. Note that this controller does not restrict the input harmonic to 2P as in other investigations (such as [3] or [17]) but includes a wider range of input harmonics (2P to 6P).

Rotor Model

The rotor model used in the study is a variant the four-bladed hingeless rotor of the BO-105 helicopter. To better capture the effects of stall control on modern rotors, two modifications are made to the baseline BO-105 rotor: (1) the HH-10 airfoil is used instead of the NACA 23012 and (2) blade linear twist is decreased from -8 to -10 deg. Beside these modifications, the blade geometry and structural properties are essentially the same as the BO-105 rotor blade. The major characteristics of the rotor model are listed in Table 1.

Flight Conditions

Simulated flight conditions with significant blade stall are selected at several forward speeds. These included a low speed condition at 63 knots ($\mu = 0.15$, $C_T/\sigma = 0.16$), cruise speed condition at 127 knots ($\mu = 0.3$, $C_T/\sigma = 0.13$), and a high speed condition at 148 knots ($\mu = 0.35$, $C_T/\sigma = 0.12$). For all flight conditions, the steady hub moments are trimmed to zero.

Results and Discussion

Open Loop Study

An open-loop study is performed to evaluate the sensitivity of the stall index to the amplitude and phase variation of single harmonic inputs. The approach consists of a phase variation of an input harmonic at a fixed amplitude and a subsequent amplitude variation about an optimum phase where the controlled parameter is at a minimum. These results provide insight into the input-output behavior of the control system and help define the type of controller (linear versus nonlinear) to use. The effectiveness of the closed-loop system is also estimated based on open-loop data. Representative results are presented in this paper.

Figure 1 shows the variation of the stall index z due to a 2P phase sweep at 1 deg excitation for the cruise speed flight condition ($\mu = 0.3$, $C_T/\sigma = 0.13$). The results indicate that the stall index varies almost linearly at this amplitude of 2P excitation. Since the phase range for minimum stall is between 180 and 270 deg, the 2P pitch

schedule for stall reduction peaks at two regions of the rotor azimuth -- one between 90 to 135 deg and the other between 270 to 315 deg. This result is rather counter-intuitive since Fig. 2(a), which shows the plot of the excess lift (F in Eq. 4) over the rotor disk, indicates that stall occurs between 270 and 300 deg azimuth. Interestingly, Fig. 2(b), which shows the stall behavior at 240 deg of 2P phase, indicates that the rotor is almost stall-free. These results imply that the blade aeroelastic responses to higher harmonic input are important considerations in stall suppression for helicopters.

The effects of 2P amplitude variation at 240 deg phase on the stall index are shown in Figure 3 for the cruise speed flight condition. The results indicate that the stall index increases with 2P amplitude above 1 deg at this phase angle. Curve-fitting the results indicates an optimum amplitude at roughly 0.9 deg at this phase angle.

For the 2P phase sweep at the same operating condition, the shaft torque variation exhibits a different trend than that of the stall index. The results are shown in Fig. 4. Although the relative change in shaft torque is small compared to the change in stall index, a 2 percent reduction in shaft torque is, however, a significant gain in rotor performance. While minimum stall index occurs in the range of 180 to 270 phase angle (Fig. 1), minimum torque is at 30 deg phase. In fact, in the phase region where stall index is minimum (180 to 270 deg), the rotor shaft torque increases above the uncontrolled value and even reaches a maximum at 210 deg phase. An explanation of this phenomenon is provided by an investigation of Fig. 5. Figures 5(a)-5(c) show the evolution of the blade drag coefficient over the rotor disk for the baseline case, minimum stall index case, and minimum shaft torque case, respectively. The results show that the drag behavior along the entire blade span shown in the region near 300 deg azimuth is responsible for this phenomenon. Of the three cases shown, the minimum stall index case has the highest drag rise, while minimum torque has a drag reduction from the baseline. Since the stall area is localized inboard, reducing stall does not guarantee an improvement in rotor performance.

Open loop results for the low speed flight condition ($\mu = 0.15$, $C_T/\sigma = 0.16$) are shown in Fig. 6. The sensitivity of the stall index to 2P excitation is weak. Figure 6(a) shows that the stall index varies by only 20 percent with the 2P phase sweep at 1 deg amplitude. The shaft torque variation with the same phase sweep is moderate, however, varying by 6 percent about the uncontrolled value. The amplitude variation at the phase for minimum stall index (330 deg) shown in Fig. 6(b) exhibits the same low sensitivity. At this low speed condition, the stall index can be reduced, at best, by only 10 percent with 2 deg of 2P input. Open loop results for other harmonics show similar results -- the stall index is fairly insensitive

to higher harmonic control at this low speed flight condition.

Closed Loop Study

Closed loop results for the low speed flight condition ($\mu = 0.15$, $C_T/\sigma = 0.16$) are presented first. Input harmonics from 2P to 4P are used; the 5P and 6P components are found to de-stabilized the closed-loop operation at this flight condition. The controller reduces the stall index by 17 percent, with a control amplitude (root-mean-square value) of 0.6 deg. The stall behavior for the uncontrolled and controlled cases are shown in Figs. 7(a) and 7(b), respectively. Compared to the uncontrolled case, the controlled excess lift (stall) region is narrower in azimuth range, yet protrudes slightly outboard. For this flight condition, the stall index reduction is accompanied by an 8.5 percent reduction in shaft torque. The input for stall suppression at this flight condition is shown as Case 1 in Table 2.

For the cruise speed flight condition ($\mu = 0.3$, $C_T/\sigma = 0.13$), the controller uses input harmonics from 2P to 6P. The stall index is reduced by over 75 percent, and the control amplitude is only 0.37 deg. Table 2 shows the amplitudes and phases of the blade pitch harmonics (Case 2). For the same flight condition, the open loop results shown previously that the same level of stall alleviation can be achieved with 1.0 deg of 2P input, and yet the shaft torque increases. For the multi-harmonic case, however, the reduction in stall is accompanied by a 0.5 percent reduction in shaft torque. With multi-harmonic inputs, Fig. 8 shows that stall can be reduced without increasing the blade drag in the azimuth region of 300 deg (compare Fig. 8 with Figs. 5(a), (b)).

Effectiveness of the closed loop operation using only 2P is evaluated. The controller converges to a minimum stall index using 0.85 deg of control amplitude at 220 deg phase (Table 2, Case 3). The reduction in stall is similar to the multi-harmonic cases, achieving a 74 percent reduction in stall index. As in the open loop results, the 2P input increases the rotor shaft torque by 2.3 percent. For stall suppression, multi-harmonic inputs are more efficient than 2P input in terms of control amplitude requirement. Furthermore, the multi-harmonic input incurs no performance penalty.

Closed-loop control with multi-harmonic input is also effective at the high speed condition ($\mu = 0.35$, $C_T/\sigma = 0.12$). Since the system exhibits moderately nonlinear behaviors, this is the only flight condition that requires transfer matrix updating. The stall index is reduced by 75 percent using 0.8 deg of control amplitude (see Table 2, Case 4). Figures 9(a) and 9(b) show the stall behavior for the uncontrolled and controlled cases, respectively. All the stall areas, except for the one at the advancing blade tip region, are suppressed. The blade drag plots of

Fig. 10 show that the controller is capable of relieving most of the drag rises over the rotor disk, resulting in 6 percent reduction in the rotor shaft torque.

Control for Performance Gain

For this part of the study, the rotor shaft torque is the controlled parameter. The cruise speed flight condition is considered ($\mu = 0.3$, $C_T/\sigma = 0.13$). The controller employs a multi-harmonic input including 2P to 6P components. The controller reduces the shaft torque by 5 percent. The maximum control authority was roughly 0.6 deg with the 3P and 4P components dominant (see Table 2, Case 5). The stall index, however, increased by 1 percent. A comparison of two multi-harmonic waveforms -- one for stall suppression (Case 2) and one for torque reduction (Case 5) -- at the same flight condition is shown in Fig. 11. An explanation for the difference in control waveforms is that for performance improvement, the input requirement is global, encompassing many different phenomena such as retreating blade stall and advancing blade compressibility. On the other hand, the requirement for stall index suppression is local, focusing only on the stall region on the retreating side.

Concluding Remarks

The results of this investigation demonstrated that stall can be suppressed effectively with higher harmonic control at both cruise and high speed flight conditions. The control amplitude requirements are less than 1 deg. However, since stall is only one of the phenomena affecting rotor performance, stall index suppression, as implemented here, does not guarantee a gain in rotor performance.

In low speed flight, open loop results indicate that the stall index was fairly insensitive to higher harmonic input. Although the reduction in stall index was small with the closed loop multi-harmonic control, a sizable gain in rotor performance was achieved.

The blade pitch schedule that improved rotor performance was different from the one that suppressed stall for the cruise speed flight condition. Rotor performance improvement can be achieved, in fact, with a small degradation in stall behavior.

References

1. Gessow, A. and Myers, C. *Aerodynamics of the Helicopter*. Frederick Ungar, New York, NY, 1981.
2. McCroskey, W. J., "Some Current Research in Unsteady Fluid Dynamics," *Journal of Fluid Engineering*, Vol. 99, Mar 1977.
3. Jacklin, S., Nguyen, K., Blaas, A., Richter, P., "Full Scale Wind tunnel Test of a Helicopter Individual Blade Control System," Proceedings of the 50th Annual Forum

of the American Helicopter Society, Washington DC, May 1994.

4. Stewart, W., "Second Harmonic Control on the Helicopter Rotor," Aeronautical Research Council, Reports and Memoranda Number 2997, Aug 1952.
5. Payne, P. R., "Higher Harmonic Rotor Control," *Aircraft Engineering*, Vol. 30, (354), Aug 1958.
6. Arcidiacono, P. J., "Theoretical Performance of Helicopters Having Second and Higher Harmonic Feathering Control," *Journal of the American Helicopter Society*, Vol. 6, (2), Apr 1961.
7. Drees, J. M. and Wernicke, R. K., "An Experimental Investigation of a Second Harmonic Feathering Device on the UH-1A Helicopter," U.S. Army Transportation Research Command, TR-62-109, Fort Eustis, VA, Jun 1963.
8. Kretz, M., "Active Eliminating of Stall Conditions," Proceedings of the 37th Annual Forum of the American Helicopter Society, New Orleans, LA, May 1981.
9. Kretz, M., "Active Expansion of Helicopter Flight Envelope," Proceedings of the Fifteenth European Rotorcraft and Powered Lift Aircraft Forum, Amsterdam, The Netherlands, Sep 1989.
10. Ham, N. and Quackenbush, T., "A Simple System for Helicopter Individual-Blade-Control and Its Application to Stall Flutter Suppression," Proceedings of the Seventh European Rotorcraft and Powered Lift Aircraft Forum, Garmish-Partenkirchen, Germany, Sep 1981.
11. Ham, N., "Helicopter Stall Alleviation Using Individual-Blade-Control," Proceedings of the Tenth European Rotorcraft and Powered Lift Aircraft Forum, The Hague, The Netherlands, Aug 1984.
12. Chopra, I. and Gunjit, S. B., "University of Maryland Advanced Rotor Code: UMARC," Proceedings of the Aeromechanics Specialists Conference, San Francisco, CA, Jan 1994.
13. Leishman, J. G., and Beddoes, T. S., "A Semi-Empirical Model for Dynamic Stall," *Journal of the American Helicopter Society*, Vol. 34, (3), Jul 1989.
14. Johnson, W., "A Comprehensive Analytical Model of Rotorcraft Aerodynamics and Dynamics, Part I: Analysis and Development," NASA TM-81182, Jun 1980.
15. Dennis, J. E., Jr. and Schnabel, R. B. *Numerical Method for Unconstrained Optimization and Nonlinear Equations*. Prentice Hall, Englewood Cliffs, NJ, 1983.
16. Nguyen, K. and Chopra, I., "Application of Higher Harmonic Control to Rotors Operating at High Speed and Thrust," *Journal of the American Helicopter Society*, Vol. 35, (3), Jul 1990.
17. Nguyen, K. and Chopra, I., "Effects of Higher Harmonic Control on Rotor Performance and Control Loads," *Journal of Aircraft*, Vol. 29, (3), May-Jun 1992.

Table 1. Blade Properties

Number of blades	4
Radius, ft	16.11
Tip speed, ft/sec	715
Tip Mach number	0.6334
Chord, in	10.63
Solidity ratio	0.0701
Root cut-out, ft	3.7
Linear twist	-10
Precone, deg	2.5
Lock number	5.40
Airfoil	HH-10
Computed blade frequencies (425 rpm, per rev)	
First lag	0.71
First flap	1.125
First torsion	3.68
Second lag	4.53
Second flap	2.82
Third flap	5.10

Table 2. Closed-Loop Results

Cases	Flight Condition	A ₂ ; φ ₂ (deg)	A ₃ ; φ ₃ (deg)	A ₄ ; φ ₄ (deg)	A ₅ ; φ ₅ (deg)	A ₆ ; φ ₆ (deg)	ΔStall Index (%)	ΔShaft Torque(%)
1	Low Speed	.10; -13	.37; 112	.98; -99	-	-	-17	-8.5
2	Cruise	.12; -140	.08; 77	.05; -143	.11; 35	.32; 125	-75	-0.5
3	Cruise	.85; -140	-	-	-	-	-74	2.3
4	High Speed	.26; 117	.30; 1	.05; 180	.47; -24	.51; 125	-75	-6
5	Cruise	.04; -56	.23; 132	.39; 31	.09; 32	.13; 13	1	-5

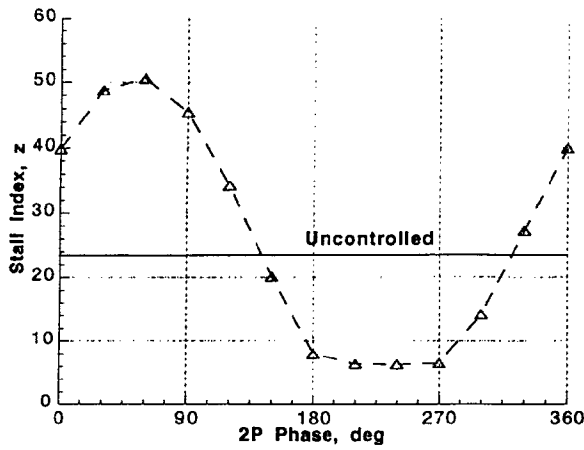


Fig. 1. Variation of stall index with 2P phase angle, 1 deg amplitude ($\mu=0.3$, $C_T/\sigma=0.13$).

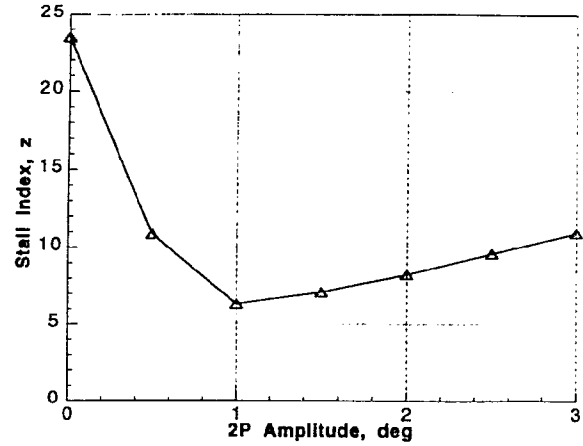
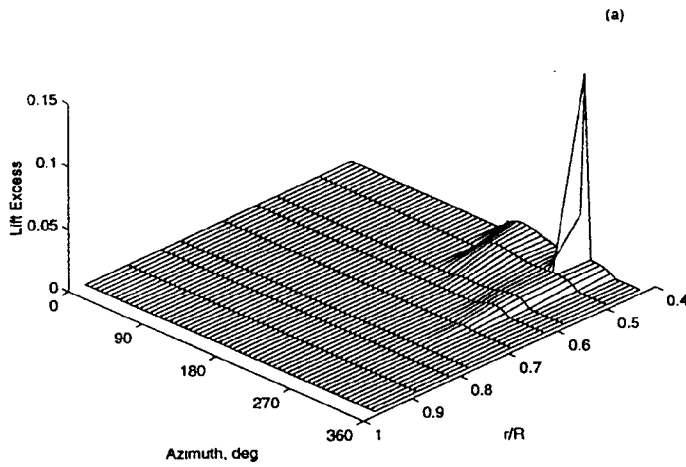


Fig. 3. Variation of stall index with 2P amplitude at 240 deg phase ($\mu=0.3$, $C_T/\sigma=0.13$).



(a)

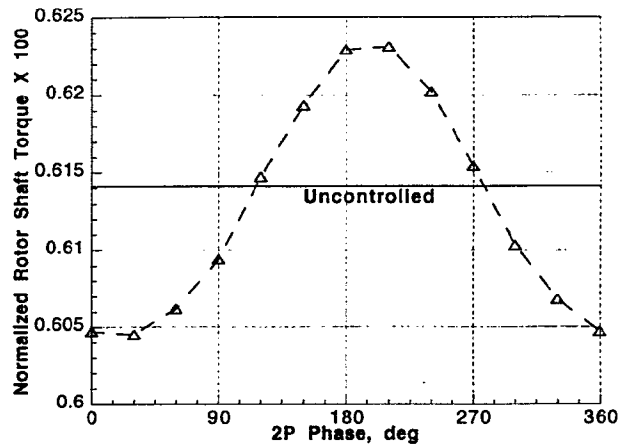
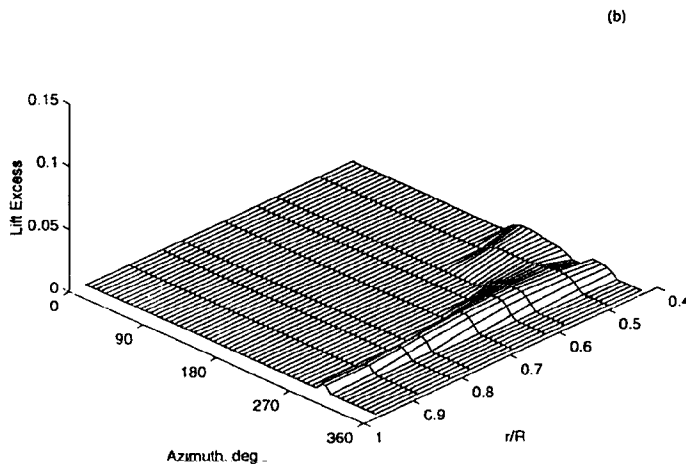
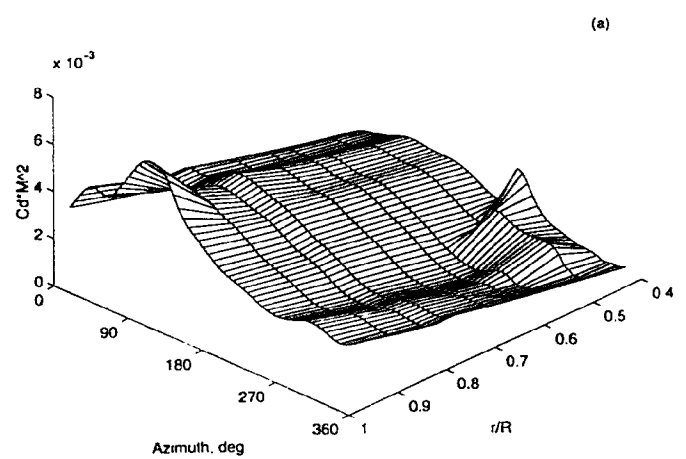


Fig. 4. Variation of shaft torque with 2P phase angle, 1 deg amplitude ($\mu=0.3$, $C_T/\sigma=0.13$).



(b)



(a)

Fig. 2. Evolution of stall over rotor disk, (a) uncontrolled, (b) 2P phase of 240 deg at 1 deg amplitude ($\mu=0.3$, $C_T/\sigma=0.13$).

Fig. 5. Evolution of blade drag over rotor disk, uncontrolled ($\mu=0.3$, $C_T/\sigma=0.13$).

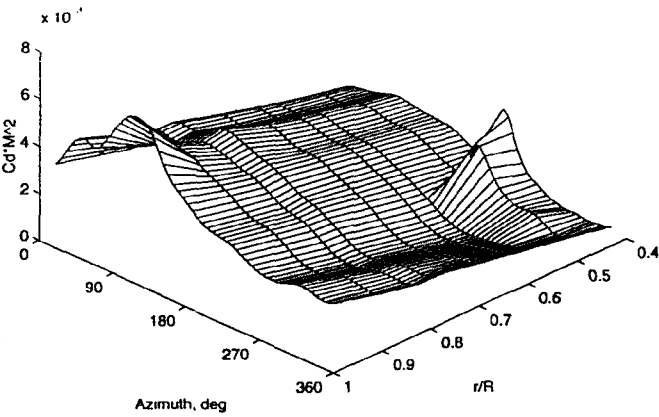
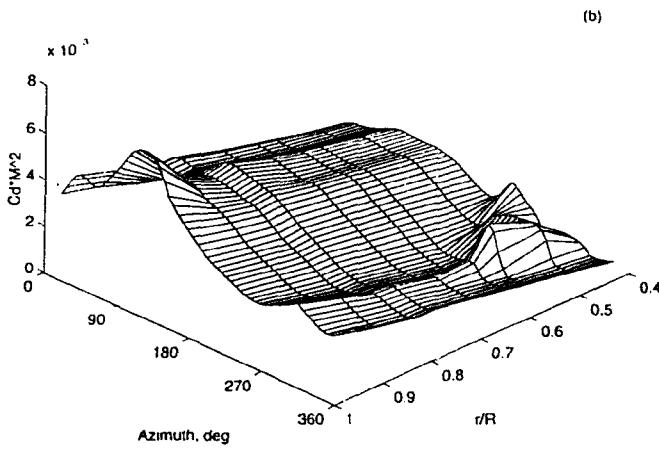


Fig. 5(cont.). Evolution of blade drag over rotor disk: (b) minimum stall (2P phase 240 deg), (c) minimum torque (2P phase 60 deg) ($\mu = 0.3$, $C_T/\sigma = 0.13$).

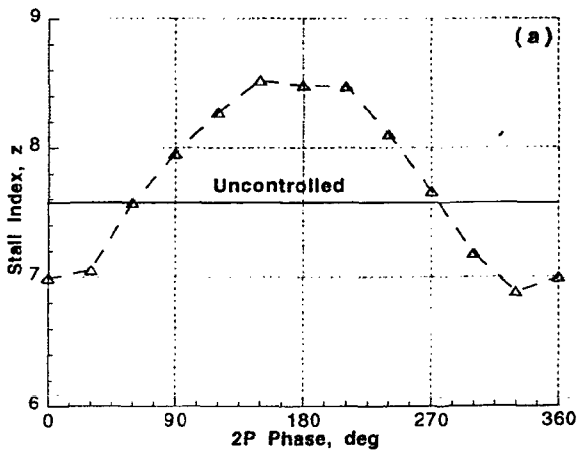


Fig. 6(a). Variation of stall index with 2P phase angle, 1 deg amplitude ($\mu = 0.15$, $C_T/\sigma = 0.16$).

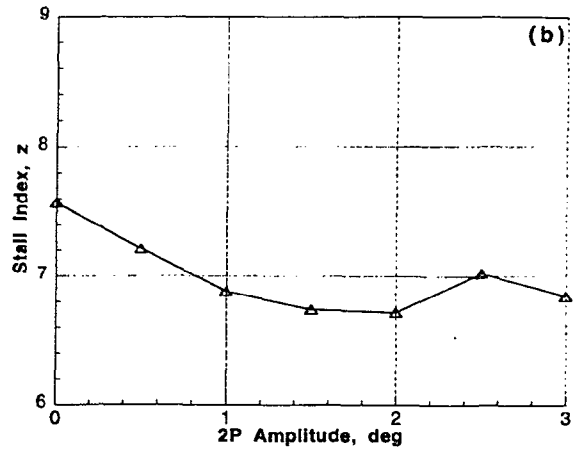


Fig. 6(b). Variation of stall index with 2P amplitude at 330 deg phase ($\mu = 0.15$, $C_T/\sigma = 0.16$).

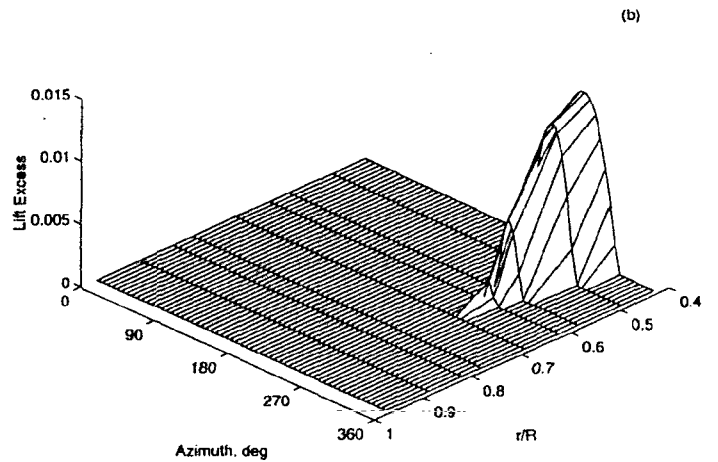
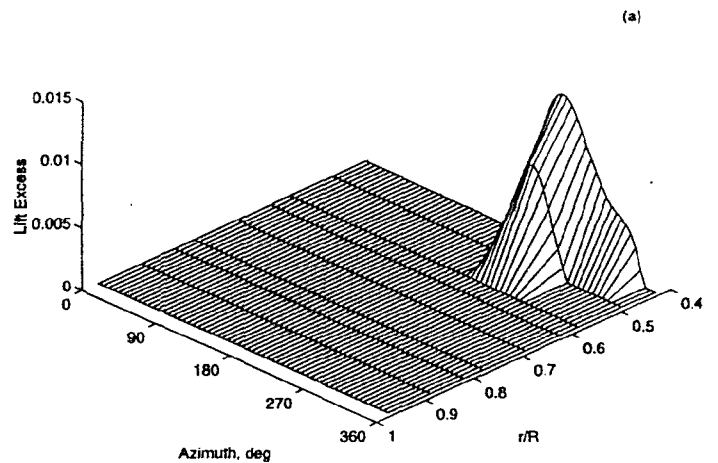


Fig. 7. Evolution of stall over rotor disk: (a) uncontrolled, (b) multi-harmonic control ($\mu = 0.15$, $C_T/\sigma = 0.16$).

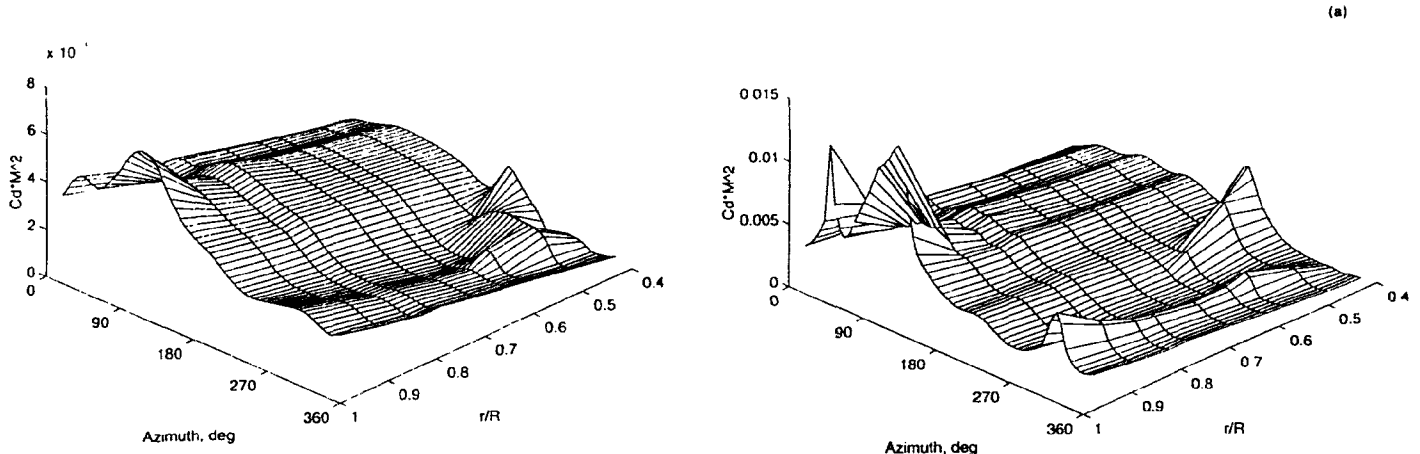


Fig. 8. Evolution of blade drag over rotor disk with multi-harmonic control ($\mu=0.3$, $C_T/\sigma = 0.13$).

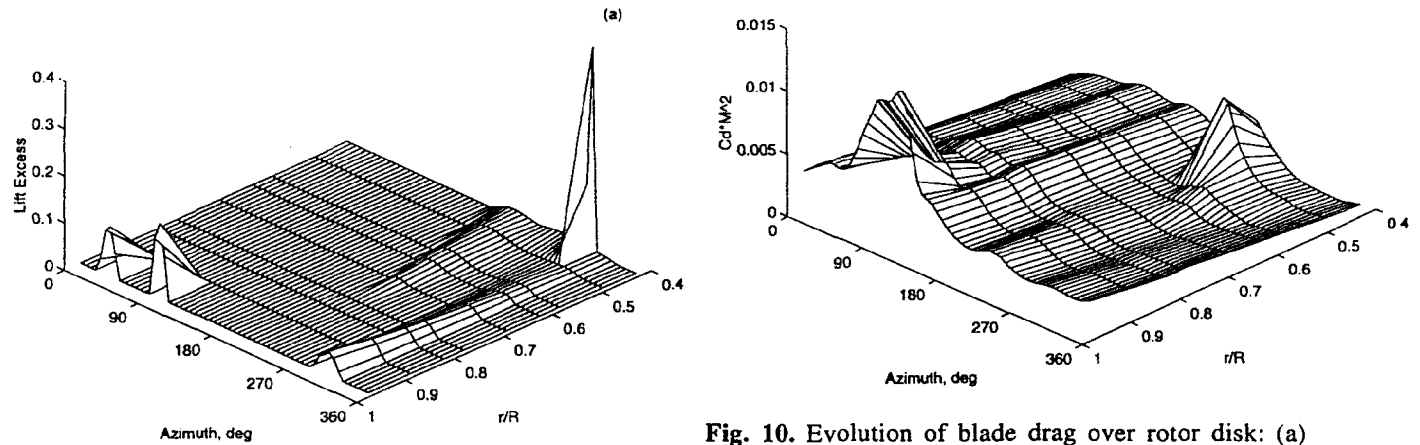


Fig. 10. Evolution of blade drag over rotor disk: (a) uncontrolled; (b) multi-harmonic control ($\mu=0.35$, $C_T/\sigma = 0.12$).

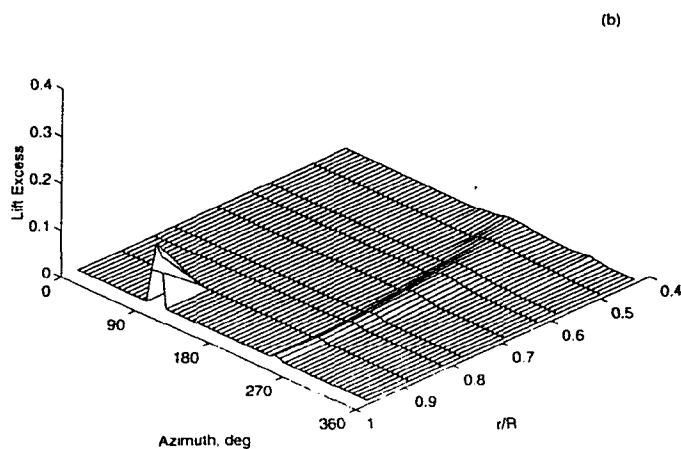


Fig. 9. Evolution of stall over rotor disk, (a) uncontrolled, (b) multi-harmonic control ($\mu=0.35$, $C_T/\sigma = 0.12$).

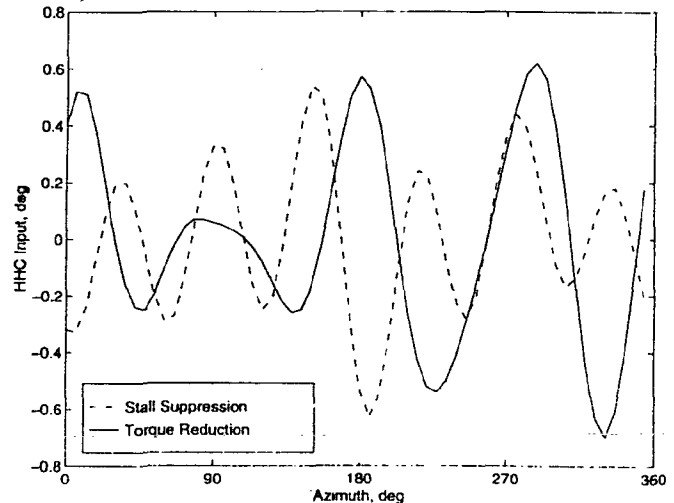


Fig. 11. Comparison of HHC schedules for stall suppression and for torque reduction, ($\mu=0.3$, $C_T/\sigma = 0.13$).